

1 **Linking glacier extent and summer temperature in NE Russia - implications**  
2 **for precipitation during the global Last Glacial Maximum**

3 **Vera D. Meyer<sup>1,2</sup> and Iestyn D. Barr<sup>3</sup>**

4 1 Alfred-Wegener-Institute, Helmholtz Centre for Polar and Marine Research, Bremerhaven,  
5 Germany

6 2 Department of Geosciences University of Bremen, Germany

7 3 School of Natural and Built Environment, Queen's University Belfast, UK

8 Corresponding author: [vera.meyer@awi.de](mailto:vera.meyer@awi.de)

9

10 **Abstract**

11 It is generally assumed that during the global Last Glacial Maximum (gLGM, i.e. 18-24 ka BP)  
12 dry climatic conditions in NE Russia inhibited the growth of large ice caps and restricted  
13 glaciers to mountain ranges. However, recent evidence has been found to suggest that glacial  
14 summers in NE Russia were as warm as at present while glaciers were more extensive than  
15 today. As a result, we hypothesize that precipitation must have been relatively high in order to  
16 compensate for the high summer temperatures and the resulting glacial ablation. We estimate  
17 precipitation abundance by mass balance calculations for the paleo-glaciers on Kamchatka and  
18 in the Kankaren Range using a degree-day-modelling (DDM) approach, and find that  
19 precipitation during the gLGM was likely comparable to, or even exceeded, the modern  
20 average. We suggest that stronger than present southerly winds over the Northwest Pacific may  
21 have accounted for the abundant precipitation. The DDM-results imply that summer  
22 temperature, rather than aridity, limited glacier extent in the southern Pacific Sector of NE  
23 Russia during the gLGM.

24

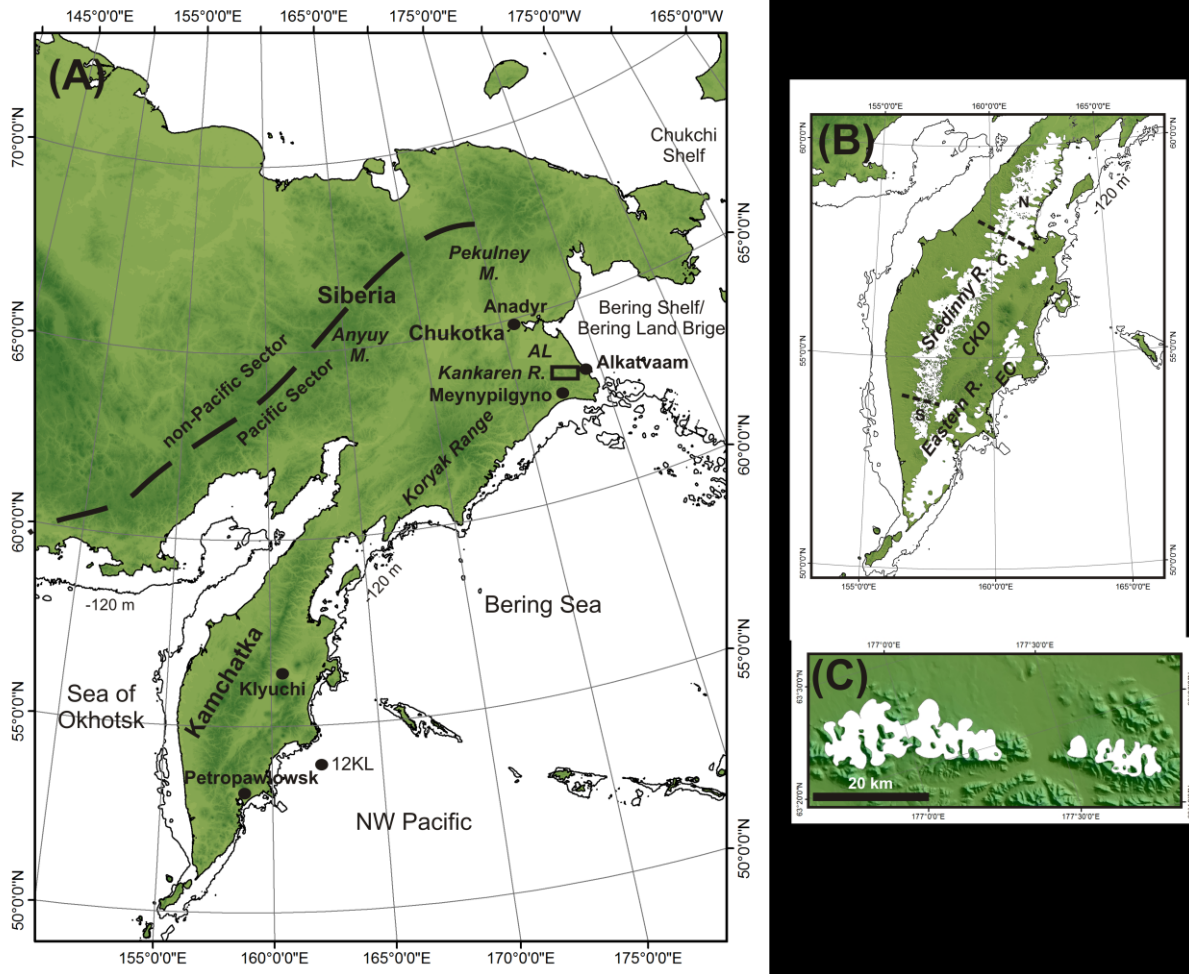
25 **Keywords:** Siberia, Last Glacial Maximum, glaciation, precipitation, summer temperature

26

## 27        1) Introduction

28    An understanding of the extent of glaciers in East Asia during the global Last Glacial Maximum  
29    (gLGM, i.e. 18-24 ka BP, Mix et al. (2001)), and an appreciation of the underlying controlling  
30    mechanisms are important for the paleoclimate modelling community, as the presence of large  
31    ice-caps during this period would strongly impact climatic conditions in the North Pacific (N  
32    Pacific) region (Felzer et al., 2001, Bigg et al., 2008). Glacier extent in Northeast Russia (NE  
33    Russia) during the gLGM has been controversially discussed in the literature. For a long time  
34    the idea that a large pan-Arctic ice sheet stretched over western Beringia (Beringia is defined  
35    as the region stretching from Siberia to Alaska) dominated the scientific debate (Grosswald,  
36    1988, 1998; Grosswald and Hughes, 2002; Grosswald and Hughes, 2005). However, this  
37    hypothesis was challenged by many studies in which Pleistocene moraines in NE Russia were  
38    dated using luminescence, cosmogenic and radiocarbon techniques. These studies provided  
39    evidence that Beringia remained largely ice-free during the gLGM, and that glaciers were  
40    restricted to mountain ranges (Velichko et al., 1984; Arkhipov et al., 1986; Glushkova, 2001;  
41    Gualtieri et al., 2000; Gualtieri et al., 2003; Brigham-Grette et al., 2003; Zamoruyev, 2004;  
42    Stauch and Gualtieri, 2008; Barr and Clark, 2012). For example, evidence was found to suggest  
43    that glaciers along the Pacific coast (e.g., in the Koryak Range and Kamchatka, Fig. 1A) were  
44    less than 80 km in length, and further inland (e.g., in the Pekulney Mountains) glaciers were  
45    even smaller, reaching a maximal length of ~ 40 km (Barr and Clark, 2012 and references  
46    therein). By now, the idea of limited mountain glaciation has become widely accepted, and it  
47    is generally supposed that the Beringian climate was too dry to allow extensive ice sheet growth  
48    during the gLGM (e.g. Brigham-Grette et al., 2003). Interestingly, several proxy-based  
49    paleoclimate studies (based on pollen, beetles and biomarkers) indicate that in Siberia, and in  
50    parts of the formerly exposed Bering Land Bridge (BLB), gLGM summers were as warm as,  
51    or even warmer than, present (Elias, 2001; Alfimov and Berman, 2001; Kienast et al., 2005;

52 Sher et al., 2005; Berman et al., 2011; Meyer et al., 2016a). This applies to many areas,  
53 including Kamchatka, a mountainous Peninsula attached to Chukotka (south-eastern Siberia;  
54 Fig. 1A, B), and the Kankaren Range, situated north of the Koryak Range (Fig. 1; Berman et  
55 al., 2011; Meyer et al., 2016a). Glacier reconstructions from these regions suggest that the local  
56 LGM occurred c.40 ka BP, and that the extent of glaciation then diminished towards the gLGM  
57 (Stauch and Gualtieri, 2008; Barr and Clark, 2012; Barr and Solomina, 2014). During the  
58 gLGM specifically, glaciation was restricted to relatively small mountain ice masses (smaller  
59 than during earlier periods of the glacial cycle), but was more extensive than during the  
60 Holocene (St. John and Krissek, 1999, Bigg et al., 2008; Barr and Clark, 2011; Barr and  
61 Solomina, 2014).



62

63

64

65

66

67

68

69

70

71

72

73

74

**Figure 1.** (A) Overview of Northeast Russia showing the regions mentioned in the text. The division into Pacific and non-Pacific sectors (dashed line) is based upon Grosswald and Kotlyakov (1969). The gLGM shore line is sketched (solid line, sea-level ~ 120 m below present). The rectangle marks the position of the Kankaren Range. Black dots indicate sites mentioned in the text. M: Mountains; R: Range; AL: Anadyr Lowland. (B) Glacier reconstruction in the Sredinny Range and the Eastern Range for the gLGM (24-18 ka BP) after Barr and Clark (2011) and Barr and Solomina (2014) and references therein. Dashed lines indicate the different sectors of the Sredinny ice field. N: northern sector, C: central sector, S: southern sector. EC: Eastern Coast; CKD: Central Kamchatka Depression; (C) Reconstructed glaciation in the Kankaren Range during the gLGM after Barr and Clark (2011).

If warm summers accompanied this gLGM mountain-glaciation, annual precipitation was probably more abundant than hitherto assumed, so that snow accumulation could compensate for ablation during warm summers. If this was the case, glacial summer temperatures would

75 have been an important limiting factor for ice-expansion in these areas during the gLGM. This  
76 would challenge the prevailing view that ice extent was limited by the region's aridity.  
77 In this paper we test this hypothesis by estimating precipitation on Kamchatka and in the  
78 Kankaren area during the gLGM by performing mass-balance calculations for paleo-glaciers  
79 in the Sredinny (Kamchatka) and Kankaren Ranges (Fig. 1). This is conducted using a degree-  
80 day-modelling approach (DDM, e.g., Laumann and Reeh, 1993; Hughes and Braithwaite,  
81 2008). These areas are the focus of our investigation, since they are locations where Barr and  
82 Clark (2011) produce chronologically and geomorphologically constrained reconstructions of  
83 gLGM glaciers.

## 84 **2) Regional setting and climate**

85 The climate in NE Russia is generally classified as strongly continental and characterized by  
86 warm summers, cold winters and severe aridity (Ivanov, 2002). A general gradient towards less  
87 extreme conditions exists from the interior towards the Pacific coast as the marine influence  
88 increases. Kamchatka and the Kankaren Range are part of the Pacific Sector (Fig. 1A) where  
89 the climate is milder and wetter than in central Siberia. The general climatic conditions in the  
90 Pacific Sector are controlled by the interplay of the major atmospheric pressure systems over  
91 the North Pacific and the East Asian Continent. The winter climate is mainly determined by  
92 the presence of the Aleutian Low over the N Pacific and the Siberian High over Siberia. This  
93 atmospheric configuration lets northerly winds predominate over East Siberia which bring  
94 cold, arctic air masses to Pacific NE Russia. In summer, the North Pacific High (NPH) develops  
95 over the N Pacific, together with the East Asian Low over the continent. Under such conditions,  
96 southerly winds drive warm and moist maritime air masses into the Pacific Sector (Mock et al.,  
97 1998; Shahgedanova et al., 2002; Yanase and Abe-Ouchi, 2007).

98

99 *2.1. Kamchatka Peninsula/Sredinny Range*

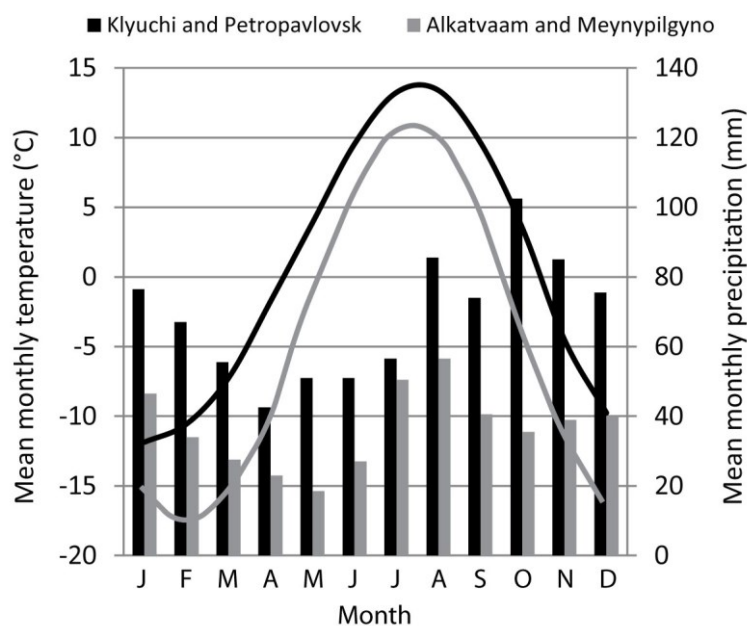
100 Kamchatka is bordered by the Sea of Okhotsk to the West, the Northwest Pacific (NW Pacific)  
101 to the Southeast and the Bering Sea to the East (Fig. 1 A). Its topography is characterized by  
102 strong variations in relief, with lowlands along the coast and in the interior (Central Kamchatka  
103 Depression, CKD), and two major mountain ranges, the Sredinny Range and the Eastern Range  
104 (Fig. 1B). The Sredinny Range reaches a maximal altitude of 3621 m above sea-level (a.s.l.).  
105 The general climate of Kamchatka is cold maritime with cool and wet summers and mild,  
106 snowy winters (Dirksen et al., 2013). Mean July and January temperatures for the entire  
107 Peninsula range from 10 to 15°C and from -8 to -26°C, respectively (Ivanov, 2002) (see Fig.  
108 2). In the coastal areas, precipitation is abundant throughout the year, e.g. 1010 mm yr<sup>-1</sup> at  
109 Petropavlovsk climate station (52.99°N, 158.66°E; Fig. 1A and 2). In interior valleys,  
110 precipitation is lower (~ 300 mm yr<sup>-1</sup>) as the Mountain Ranges shield the marine influences.  
111 Klyuchi climate station (56.32°N, 160.83°E, Fig. 1A) notes average precipitation of 635 mm  
112 yr<sup>-1</sup> (Fig. 2) but values as low as ~ 300 mm yr<sup>-1</sup> have been reported for the CKD (Ivanov, 2002;  
113 Dirksen et al., 2013). Precipitation is highest in the mountain ranges where values typically  
114 vary between 1200 mm yr<sup>-1</sup> and 1500 mm yr<sup>-1</sup> (Ivanov, 2002; Dirksen et al., 2013).

115 Today, small glaciers are only present on the highest peaks (Solomina and Calkin, 2003;  
116 Ananicheva et al., 2008; Lynch et al., 2016). A glacier reconstruction by Barr and Clark (2011)  
117 suggests that during the gLGM a continuous, mountain-centred ice field existed in the Sredinny  
118 Mountains (Fig. 1B). Its outlet glaciers extended up to 80 km into surrounding valleys, and the  
119 ice-field covered 57,363 km<sup>2</sup> (Barr and Clark, 2011). End-moraines of potential gLGM age  
120 also exist in the Eastern Range. However, since accurate dates to clearly ascribe these Eastern  
121 Range moraines to the gLGM are missing (Barr and Solomina, 2014), this paper focusses on  
122 the Sredinny Range, rather than Kamchatka as a whole.

123

124 2.2. The Kankaren Range and adjacent lowlands

125 The Kankaren Range is attached to the northern flanks of the Koryak Range and faces the  
126 Anadyr-Lowlands (AL) in the North (Fig. 1A). The Kankaren Mountains reach maximal  
127 altitudes of 1200 m a.s.l.. Direct observations of modern climate conditions in the mountains  
128 themselves are lacking. The closest climate stations are in Alkatvaam (63.133°N, 179.03°E)  
129 and Meynypilgyno (62.54°N, 177.05°E; Fig. 1A), respectively, ~ 60 km East, and ~ 85 km  
130 South of the Kankaren Mountains, where average July, January and annual temperatures  
131 (10.8°C, -15.7°C and -5.2°C) are typically lower than on Kamchatka (see Fig. 2). Precipitation  
132 values for the Kankaren Range are also lacking, though the data from Alkatvaam and  
133 Meynypilgyno suggest modern precipitation of ~ 439 mm yr<sup>-1</sup> (<http://de.climate-data.org>).  
134 According to the glacier reconstruction by Barr and Clark (2011), the western part of the  
135 Kankaren Range was covered by a mountain-centred ice-field during the gLGM, while the  
136 eastern sector was occupied by a group of five valley glaciers (Fig. 1C). This reconstruction  
137 reveals glaciers up to 7 km in length and a total ice covered area of 215 km<sup>2</sup>. By contrast, the  
138 mountains are currently glacier free.



139

140 **Figure 2.** Modern climate data averaged for stations in Klyuchi and Petropavlovsk (for Kamchatka/the Sredinny Range), and  
141 Alkatvaam and Meynypilgyno (for the Kankaren Range). These data were taken from (<http://en.climate-data.org>) and are  
142 corrected to sea level using a lapse-rate of 0.63°C/100 m.

### 143 **3) Degree Day Modelling**

#### 144 *3.1. General Model setup*

145 In order to estimate the accumulation necessary to sustain the reconstructed gLGM glaciers in  
146 the Sredinny and Kankaren Ranges (reconstruction from Barr and Clark, 2011), given summer  
147 temperatures equivalent to modern, we applied a degree day modelling (DDM) approach –  
148 allowing the annual accumulation needed to balance annual ablation at the equilibrium line  
149 altitudes (ELAs) of former glaciers to be estimated (Laumann and Reeh, 1993; Braithwaite et  
150 al., 2006). A glacier’s ELA is defined as the altitude where net annual accumulation and  
151 ablation are in equilibrium, and is largely controlled by climate (Ohmura et al., 1992). In the  
152 DDM approach, the annual melt at the glacier’s ELA is calculated from the sum of daily melt  
153 values ( $M_d$ ). Each  $M_d$  can be calculated as a function of daily mean temperature (where  
154 positive) at the paleo-ELA ( $T_d$ ; eq. 1) and a degree-day melt factor (DDF; eq. 1). In this study  
155 DDFs of 4.0 and 2.5 mm d<sup>-1</sup> °C<sup>-1</sup> are used (Braithwaite et al., 2006). The former is based on  
156 the assumption that gLGM glaciers were temperate (with high mass-flux), and the latter on the  
157 assumption that they were of polar type (with low mass-flux).

$$158 \quad M_d = T_d * DDF \quad (\text{eq. 1})$$

159 The annual sum of these daily melt values is then assumed to be equalled by accumulation  
160 (expressed in mm) at the ELA (since, at the ELA, annual accumulation = annual ablation).

161 Assuming that the annual distribution of temperatures is described by a sine curve, (Brugger,  
162 2006; Hughes, 2008, 2009; Hughes and Braithwaite, 2008) daily temperatures at the paleo-  
163 ELA can be calculated from mean annual air temperature at the paleo-ELA as follows (eq. 2):



164 
$$T_d = A_y \sin\left(\frac{2\pi d}{\lambda} - \phi\right) + T_a \quad (\text{eq. 2}),$$

165 where  $A_y$  is the amplitude of annual temperature variability (1/2 of the annual temperature  
166 range),  $d$  the ordinal day,  $\lambda$  is the period (365 days),  $\phi$  is the phase angle of the sine curve (here  
167 1.93 radians based on the general assumption that temperature is maximal in July and minimal  
168 in January), and  $T_a$  is mean annual air temperature.

### 169 *3.2. Setup of simulated scenarios for Kamchatka and in the Kankaren Range*

170 In order to estimate the gLGM accumulation for the Sredinny and the Kankaren mountain  
171 ranges, the DDM was applied to paleo-ELA data from Barr and Clark (2011). For the Sredinny  
172 Range, the model was run with the mean ELA of the entire Sredinny ice-field and with average  
173 ELAs of the southern, central and northern sectors of the ice field (Fig. 1B). The division was  
174 implemented as the ELA-reconstruction by Barr and Clark (2011) yielded a north-south  
175 gradient with a decrease in ELAs towards the north. In the Kankaren Range, an ELA gradient  
176 was not reconstructed rendering a separation into sectors not necessary. The DDM was applied  
177 only to the mean ELA of the entire glacier-field (Fig. 1C). gLGM conditions were simulated  
178 assuming that glacial mean July temperatures ( $T_{\text{July}}$ ) equal modern values (Alfimov and  
179 Berman, 2001; Berman et al., 2011; Meyer et al., 2016a), but winters were colder than at  
180 present (Meyer et al., 2002), conditions yielding a larger  $A_y$  compared to today.

181 In order to simulate LGM temperatures ( $T_d$ , eq. 2) for the Sredinny and Kankaren ranges, the  
182 perturbation in mean annual temperature during the gLGM relative to pre-industrial conditions  
183 ( $\Delta T_{a \text{ LGM}}$ ) was calculated from climate-model data (Kim et al., 2008) since, to our knowledge,  
184 no proxy-based absolute estimates of mean annual temperature during the gLGM exist for the  
185 Kankaren or Sredinny Ranges. For eastern Siberia as a whole, the climate-model suggests a  
186  $\Delta T_{a \text{ LGM}}$  of  $\sim 6\text{-}14^\circ\text{C}$  (Kim et al., 2008). If  $T_{\text{July}}$  during the gLGM is known (assumed to equal  
187 modern),  $A_y$  at the LGM ( $A_{y \text{ LGM}}$  needed to calculate daily temperatures, eq. 2) can be

188 approximated by eq. 3 (again, assuming that the annual distribution of temperatures is  
 189 described by a sine curve with July and January being the warmest and coldest months of the  
 190 year):

$$191 \quad A_y = T_{\text{July}} - T_a \quad (\text{eq. 3})$$

192 Modern  $T_{\text{July}}$  and  $T_a$  for Kamchatka were calculated by combining data from Klyuchi and  
 193 Petropavlovsk climate stations (Fig. 1A and 2). The stations represent the continental climate  
 194 of the CKD and the maritime conditions at the Eastern Coast (<http://en.climate-data.org>)— the  
 195 areas most relevant to palaeotemperature reconstructions from Meyer et al. (2016a). The  
 196 averaged data from these two climate stations indicate modern July, January and annual  
 197 temperatures of 13.1°C, -12.0°C, and 0.4°C, respectively (see Fig. 2). Correcting these data for  
 198 altitude, using a lapse-rate of 0.63°C/100 m (Osipov, 2004), gives a modern sea level  $T_{\text{July}}$  and  
 199  $T_a$  of 13.2°C and 0.6°C, respectively, and an  $A_y$  of 12.6°C (based on mean monthly values)  
 200 (see Fig. 2 and Table 1). Modern  $T_{\text{July}}$  and  $T_a$  for the Kankaren Range were calculated by  
 201 combining data from Alkatvaam and Meynypilgyno climate stations (Fig. 1A). Correcting  
 202 these data for altitude reveals modern sea level  $T_{\text{July}}$  and  $T_a$  values of 10.9°C and -5.1°C,  
 203 respectively (see Fig. 2 and Table 1).

204 **Table 1.** Modern mean July and annual temperatures and amplitudes of the annual temperature cycle in Kamchatka and  
 205 the Kankaren area. The data were taken from Klyuchi and Petropawlovsck (Sredinny Range) and Alkatvaam and  
 206 Meynypilgyno climate stations (Kankaren Range) and were corrected to sea level using a lapse-rate of 0.0063°C/m.

Modern at s. l.	Sredinny Range	Kankaren Range
$T_{\text{July}}[\text{°C}]$	13.3	10.9
$T_a[\text{°C}]$	0.6	-5.1
$A_y[\text{°C}]$	12.7	16.0

210 Kim et al. (2008), we considered gLGM climate scenarios for both the minimal and maximal  
 211  $\Delta T_a$  LGM estimates (see Table 2). In addition, as the modern temperature data reflect the

212 conditions at sea-level,  $T_a$  was lowered using a lapse-rate of  $0.63^\circ\text{C}/100\text{ m}$  (Osipov, 2004) in  
213 order to obtain air temperature data at the paleo-ELAs of the gLGM glaciers reconstructed by  
214 Barr and Clark (2011) (see Tables 2 and 3). DDM-derived estimates for gLGM precipitation  
215 are given as absolute values in  $\text{mm yr}^{-1}$  and in percentage relative to modern using the range of  
216  $1200\text{-}1500\text{ mm yr}^{-1}$  (Ivanov, 2002; Dirksen et al., 2013).

## 217 **4. Results**

### 218 *4.1. Simulated summer and winter temperature at the gLGM*

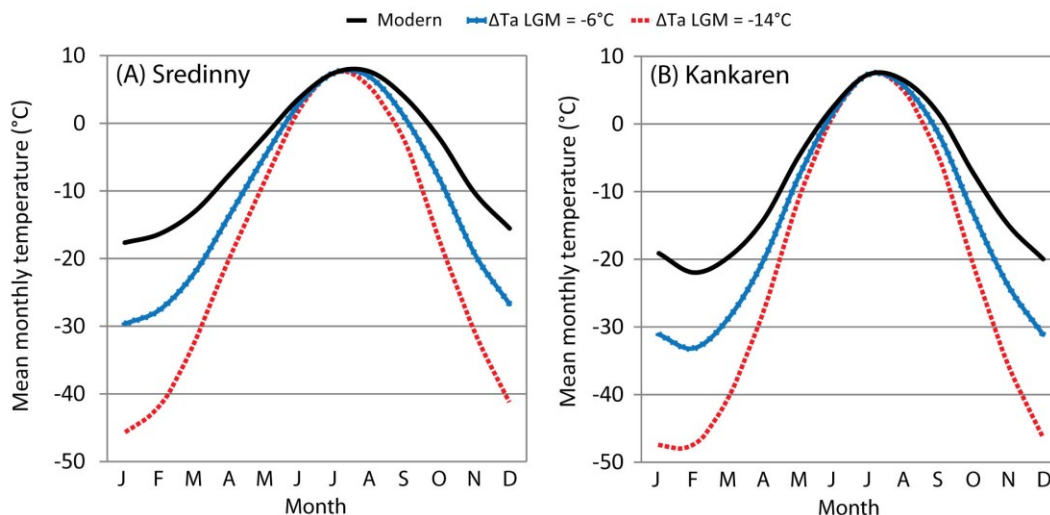
219 Given that the model runs are based on modern  $T_{\text{July}}$ , but enforce a 6 to  $14^\circ\text{C}$  reduction in mean  
220  $T_a$ ,  $A_{y\text{ LGM}}$  increases correspondingly (see eq. 3 and Fig. 3). In order to keep  $T_{\text{July}}$  at modern  
221 values,  $A_{y\text{ LGM}}$  increases in equal but inverse value with  $\Delta T_{a\text{ LGM}}$  (as it decreases). As a result,  
222 at the mean ELA of the Sredinny ice field,  $A_{y\text{ LGM}}$  varies from  $18.6^\circ\text{C}$  to  $26.6^\circ\text{C}$ , based on  
223  $\Delta T_{a\text{ LGM}}$  values of  $-6^\circ\text{C}$  and  $-14^\circ\text{C}$ , respectively (see Fig. 3). This results in mean January  
224 temperatures ( $T_{\text{Jan.}}$ ) as low as  $-29.5^\circ\text{C}$  and  $-45.5^\circ\text{C}$  during the gLGM ( $12^\circ\text{C}$  and  $28^\circ\text{C}$  below  
225 modern values) (Fig. 3A). Similarly, in the Kankaren Range,  $A_{y\text{ LGM}}$  varies from  $22.0^\circ\text{C}$  to  
226  $30.0^\circ\text{C}$ , based on  $\Delta T_{a\text{ LGM}}$  values of  $-6^\circ\text{C}$  and  $-14^\circ\text{C}$ , respectively (see Fig. 3), resulting in mean  
227  $T_{\text{Jan.}}$  of  $-31.2^\circ\text{C}$  and  $-47.2^\circ\text{C}$  during the gLGM ( $12^\circ\text{C}$  and  $28^\circ\text{C}$  below modern values) (Fig. 3B).  
228 In the Sredinny as well the Kankaran Range the number of positive degree days obtained for  
229 the gLGM using both  $\Delta T_{a\text{ LGM}}$  values of  $-6^\circ\text{C}$  and  $-14^\circ\text{C}$ , is smaller than at present.  $\Delta T_{a\text{ LGM}}$  of  
230  $-14^\circ\text{C}$  yields the fewest positive degree days (Fig. 3).

231

### 232 *4.2. Annual accumulation/precipitation*

233 The DDM-derived estimates of total annual accumulation and the duration of the ablation  
234 season (days with positive degree days) given  $\Delta T_{a\text{ LGM}}$  values of  $-6$  and  $-14^\circ\text{C}$  for temperate  
235 glaciers (DDF of 4.0) are shown in Table 2 and for glaciers of polar type (DDF of 2.5) in Table

236 3. It is worth noting that these estimates of annual accumulation do not represent direct  
 237 estimates of former annual precipitation, since the latter also includes precipitation (likely  
 238 falling as rain) during the ablation/summer season (not included in the output of the DDM).  
 239 However, since the gLGM ablation season in each of our scenarios is relatively short (ranging  
 240 between 71 and 113 days; see Tables 2 and 3), and because the DDM model fails to account  
 241 for the contribution of accumulating snow and ice from non-direct sources (i.e., windblown  
 242 and/or avalanched snow and ice from the surrounding landscape), which can be significant in  
 243 some cases (see Kern and László, 2010), the accumulation estimates derived here are regarded  
 244 as rough estimates of annual precipitation.



245  
 246 **Figure 3.** Modern and modelled LGM temperatures at the ELAs of LGM glaciers in (A) the Sredinny (ELA = 897 m.a.s.l.)  
 247 and (B) Kankaren (ELA = 575 m.a.s.l.) mountain ranges (ELA estimates based on Barr and Clark, 2011). Modern climate  
 248 data (plotted in black) is derived from climate stations in Klyuchi and Petropavlovsk (for the Sredinny Range), and  
 249 Alkatvaam and Meynypilgyno (for the Kankaren Range), and is corrected to the LGM ELAs using a lapse-rate of  
 250 0.63°C/100 m. Climate conditions at the LGM are modelled assuming perturbations in mean annual temperature ( $\Delta T_{a\text{LGM}}$ )  
 251 of -6°C and -14°C, as predicted by the climate model of Kim et al. (2008).

252  
 253 *4.2.1. Sredinny Range*

254 Modelled estimates of gLGM precipitation in the Sredinny Range based on a  $\Delta T_{a\text{LGM}}$  of -14°C  
 255 (1479-1986 mm yr<sup>-1</sup>) are always lower than their equivalents based on a  $\Delta T_{a\text{LGM}}$  of -6°C (1780-

256 2394 mm yr<sup>-1</sup>; see Tables 2 and 3, Fig. 3). Precipitation is always higher for temperate glaciers  
257 (1479-2394 mm yr<sup>-1</sup>, see Table 2) than for glaciers of polar type (924-1496 mm yr<sup>-1</sup>, see Table  
258 3). Assuming temperate glaciers (DDF of 4.0), the model output suggests that 1780–2145 mm  
259 yr<sup>-1</sup> of precipitation would be necessary to sustain the mean ELA of the entire Sredinny ice  
260 field (897 m.a.s.l.), considering both  $\Delta T_{a\text{ LGM}}$  values. When compared to modern precipitation  
261 values in the mountains this constitutes a 19–79% increase in annual precipitation (Table 2).  
262 For both  $\Delta T_{a\text{ LGM}}$  values, the average ELA of the southern sector of the Sredinny ice field  
263 requires the lowest precipitation (1479–1780 mm yr<sup>-1</sup>). Values are intermediate in the central  
264 sector (1829–2203 mm yr<sup>-1</sup>), and greatest in the northern part of the ice-field (1986–2394 mm  
265 yr<sup>-1</sup>).

266 These trends are also apparent when polar-type glaciers are assumed (DDF of 2.5, Table 3),  
267 since the model suggests that 1113–1340 mm yr<sup>-1</sup> of precipitation would be necessary to sustain  
268 the mean ELA of the entire Sredinny ice field (897 m.a.s.l), constituting between a ~ 26%  
269 decrease and ~ 12% increase relative to present (Table 3, Fig. 3). Precipitation is lowest for the  
270 average ELA of the southern sector of the Sredinny ice field (924–1112 mm yr<sup>-1</sup>), values are  
271 again intermediate in the central sector (1143–1377 mm yr<sup>-1</sup>), and the ELAs of the northern  
272 sector require the greatest precipitation to sustain the glaciers in equilibrium (1241–1496 mm  
273 yr<sup>-1</sup>).

274 Considering all scenarios, maximal precipitation (2394 mm yr<sup>-1</sup>) is found for the combination  
275 of temperate glaciers, milder winters ( $\Delta T_{a\text{ LGM}}$  of -6°C) and an ELA of 808 (northern part of  
276 the ice field, Table 1). Minimal precipitation (924 mm yr<sup>-1</sup>) estimates are found in the southern  
277 sector (ELA of 1035) when colder winters and glaciers of polar type are assumed (Table 3).

278 **Table 2.** DDM temperature-setup for the LGM simulations and results for precipitation (prec.) and the length of the ablation season. The model was run with  $\Delta T_{a\text{LGM}}$  values based on climate-  
 279 model estimates from Kim et al. (2008), and with a degree-day melt factor (DDF) of 4.0 (describing temperate glaciers) assuming that LGM  $T_{\text{July}}$  was the same as at present. Percentage change  
 280 relative to modern is calculated using modern precipitation estimates of 1200 mm yr<sup>-1</sup>–1500 mm yr<sup>-1</sup> (for the Sredinny Range).

	Sredinny Range								Kankaren Range		
	Average ELA [m.a.s.l.]	1035 (south)	876 (centre)	808 (north)	897 (mean)	1035 (south)	876 (centre)	808 (north)	897 (mean)	575 (mean)	
281											
282											
283	DDF (mm d <sup>-1</sup> °C <sup>-1</sup> )	4.0	4.0	4.0	4.0	4.0	4.0	4.0	4.0	4.0	4.0
284	$T_{\text{July LGM}}^1$	6.7	7.7	8.2	7.6	6.7	7.5	8.2	7.6	7.2	7.2
285	$\Delta T_{a\text{LGM}}$ [°C]	<b>-6.0</b>	<b>-6.0</b>	<b>-6.0</b>	<b>-6.0</b>	<b>-14.0</b>	<b>-14.0</b>	<b>-14.0</b>	<b>-14.0</b>	<b>-6.0</b>	<b>-14.0</b>
286	$A_{y\text{LGM}}$ [°C]	<b>18.6</b>	<b>18.6</b>	<b>18.6</b>	<b>18.6</b>	<b>26.6</b>	<b>26.6</b>	<b>26.6</b>	<b>26.6</b>	<b>22.0</b>	<b>30.0</b>
287	$T_{a\text{LGM}}$ [°C]	-11.9	-11.1	-10.5	-11.1	-19.9	-19.1	-18.5	-19.0	-14.6	-22.7
288	Ablation [days]	102	110	113	108	84	90	93	90	88	71
289	Annual prec. [mm yr <sup>-1</sup> ]	1780	2203	2394	2145	1479	1829	1986	1781	1291	943
	Prec. change relative to modern [%] <sup>2</sup>	+18.7 + 48.8	+46.8 +83.6	+59.6 +99.5	+43.0 +78.8	-1.4 +23.3	+21.9 +52.4	+32.4 +65.5	+18.7 ± 48.4	n.a. <sup>3</sup>	n.a. <sup>3</sup>

<sup>1</sup>: calculated from modern  $T_{\text{July}}$  (Table 1) using a lapse rate of 0.0063°C/m

<sup>1</sup>: first value refers to 1500 mm yr<sup>-1</sup>, the second to 1200 mm yr<sup>-1</sup>.

<sup>2</sup>: cannot be estimated since modern precipitation data for the mountains are not available (n.a.)

290  
291  
292

**Table 3.** DDM temperature-setup for the LGM simulations and results for precipitation (prec.) and the length of the ablation season. The model was run with  $\Delta T_{a\text{ LGM}}$  values based on climate-model estimates from Kim et al. (2008), and with a degree-day melt factor (DDF) of 2.5 (describing glaciers of polar type) assuming that LGM  $T_{\text{July}}$  was the same as at present. Percentage change relative to modern is calculated using modern precipitation estimates of 1200 mm yr<sup>-1</sup>–1500 mm yr<sup>-1</sup> (for the Sredinny Range).

	Sredinny Range								Kankaren Range		
	Average ELA [m.a.s.l.]	1035 (south)	876 (centre)	808 (north)	897 (mean)	1035 (south)	876 (centre)	808 (north)	897 (mean)	575 (mean)	575 (mean)
<b>LGM conditions at ELA</b>	DDF (mm d <sup>-1</sup> °C <sup>-1</sup> )	2.5	2.5	2.5	2.5	2.5	2.5	2.5	2.5	2.5	2.5
	$T_{\text{July LGM}}^1$	6.7	7.7	8.2	7.6	6.7	7.5	8.2	7.6	7.2	7.2
	$\Delta T_{a\text{ LGM}} [^{\circ}\text{C}]$	<b>-6.0</b>	<b>-6.0</b>	<b>-6.0</b>	<b>-6.0</b>	<b>-14.0</b>	<b>-14.0</b>	<b>-14.0</b>	<b>-14.0</b>	<b>-6.0</b>	<b>-14.0</b>
	$A_{y\text{ LGM}} [^{\circ}\text{C}]$	<b>18.6</b>	<b>18.6</b>	<b>18.6</b>	<b>18.6</b>	<b>26.6</b>	<b>26.6</b>	<b>26.6</b>	<b>26.6</b>	<b>22.0</b>	<b>30.0</b>
	$T_{a\text{ LGM}} [^{\circ}\text{C}]$	-11.9	-10.9	-10.5	-11.0	-19.9	-18.9	-18.5	-19.0	-14.7	-22.7
	Ablation [days]	102	110	113	108	84	90	93	90	88	71
	Annual prec. [mm yr <sup>-1</sup> ]	1112	1377	1496	1340	924	1143	1241	1113	807	589
	Prec. change relative to modern [%] <sup>2</sup>	-25.8 -7.3	-8.2 +14.8	-0.2 +24.6	-10.6 +11.7	-38.4 -23.0	-23.8 -4.8	-17.3 +3.4	-25.8 -7.3	n.a. <sup>3</sup>	n.a. <sup>3</sup>

293  
294  
295  
296

<sup>1</sup>: calculated from modern  $T_{\text{July}}$  (Table 1) using a lapse rate of 0.0063°C/m

<sup>2</sup>: first value refers to 1500 mm yr<sup>-1</sup>, the second to 1200 mm yr<sup>-1</sup>.

<sup>3</sup>: cannot be estimated since modern precipitation data for the mountains are not available (n.a.).

297 4.2.3. *Kankaren Range*

298 In the Kankaren Range the average ELA at the gLGM was 575 m (a.s.l) according to Barr and  
299 Clark (2011). Given this value, the precipitation required to keep the glaciers in equilibrium  
300 ranges between 589 and 1291 mm yr<sup>-1</sup> considering all scenarios (different  $\Delta T_a$  and glacier  
301 types). In all scenarios, gLGM precipitation estimates are lower than in their equivalents for  
302 the Sredinny Range (see Tables 2 and 3).

303 Like in Kamchatka, estimates for gLGM precipitation assuming colder winters ( $\Delta T_{a \text{ LGM}}$  of -  
304 14°C; i.e. 589-943 mm yr<sup>-1</sup>, see Tables 2 and 3) are lower than in the scenarios based on a  $\Delta T_a$   
305 LGM of -6°C (807-1291 mm yr<sup>-1</sup>, Tables 2 and 3). Also, assuming glaciers of polar type (DDF  
306 of 2.5 mm d<sup>-1</sup> °C<sup>-1</sup>, Table 3), the precipitation required to keep the gLGM glaciers in  
307 equilibrium (i.e. 589–807 mm yr<sup>-1</sup>) is lower than for temperate glaciers (i.e. 943-1291 mm yr<sup>-1</sup>  
308 <sup>1</sup>), the same tendency found for the Sredinny Range.

309 Again, maximal precipitation is found when warm winters and temperate glaciers are assumed  
310 (1291 mm yr<sup>-1</sup>, Tables 2 and 3) while the combination of cold winters and glaciers of polar  
311 type requires the lowest precipitation to sustain the gLGM glaciers (589 mm yr<sup>-1</sup>, Tables 2 and  
312 3).

313

314 **5. Discussion**

315 *5.1. Inferences for gLGM precipitation*

316 If gLGM glaciers in Kamchatka are assumed to have been temperate (with a DDF of 4.0 mm  
317 d<sup>-1</sup> °C<sup>-1</sup>), model scenarios generally suggest increased mean annual precipitation at the gLGM  
318 relative to modern conditions (with estimates suggesting a change of between +18.7% to  
319 +99.5% relative to modern values; see Table 2). The southern sector of the Sredinny ice-field,  
320 where ELA is highest, is an exception when  $\Delta T_{a \text{ LGM}}$  of -14°C, and hence colder winters, are



321 assumed, as the modelled value (i.e. 1479 mm yr<sup>-1</sup>) is slightly lower than 1500 mm yr<sup>-1</sup> (Table  
322 2) suggesting precipitation equalled the modern mean.

323 If glaciers are assumed to have been of polar type (i.e., with a DDF of 2.5 mm d<sup>-1</sup> °C<sup>-1</sup>), then  
324 less mean annual precipitation than for temperate glaciers is needed to sustain the glaciers at  
325 the gLGM. Precipitation is similar to modern values as the majority of the estimates for the  
326 central and northern Sredinny ice field adopted from the DDM fall in the range of modern  
327 precipitation (1200-1500 mm yr<sup>-1</sup>, see Table 3). The two scenarios assuming polar-type glaciers  
328 in the southern sector yield values below the modern range. When  $\Delta T_{a\text{LGM}}$  of -6°C is assumed  
329 (i.e. relatively warm winters) precipitation (1113 mm yr<sup>-1</sup>) is slightly below the low end of the  
330 modern range (1200 mm yr<sup>-1</sup>), It is even reduced by ~ 23 to ~ 38% (924 mm yr<sup>-1</sup>), relative to  
331 present, for  $\Delta T_{a\text{LGM}}$  of -14°C (relatively cold winters). In the central part of the ice field (ELA  
332 808 m a.s.l.) precipitation (1143 mm yr<sup>-1</sup>; Table 3) is reduced relative to present, though very  
333 close to the lower end of the modern range (1200 mm yr<sup>-1</sup>). This indicates that in combination  
334 with polar-type glaciers severe winters ( $T_{\text{Jan}}$  of -45.5°C at mean ELA;  $A_{y\text{LGM}}$  of 26.6 °C) may  
335 have allowed glaciers of the southern Sredinny ice field to be in equilibrium conditions when  
336 precipitation was significantly (>10% relative to 1200 mm yr<sup>-1</sup>) reduced relative to present  
337 while summers were as warm as today. In the central and northern part of Sredinny ice field  
338 because gLGM precipitation must have equalled modern values, despite reduced winter  
339 temperatures.

340 In the Kankaren Range the model suggests gLGM precipitation exceeds the modern value  
341 averaged from Alkatvaam and Meynypilgyno climate stations (~ 439 mm yr<sup>-1</sup>) by about 34-  
342 194%. However, these lowland stations are not representative of mountain conditions, as  
343 precipitation usually increases with altitude. So, the lack of robust information about modern  
344 precipitation in the Kankaren Range prevents direct comparison with modern values in the  
345 mountains. However, the difference between our estimates for gLGM precipitation in the

346 Sredinny and Kankaren ranges ( $\sim 500 \text{ mm yr}^{-1}$ ) is similar to the modern deviation between  
347 averaged values for Alkatvaam and Meynypilgyno climate stations ( $\sim 439 \text{ mm yr}^{-1}$ ) and the  
348 value compiled from Klyuchi and Petropawlowsk ( $\sim 823 \text{ mm yr}^{-1}$ ). Considering this, the DDM  
349 results imply that sign and magnitude of gLGM-to-Holocene precipitation changes may have  
350 been similar in both areas (i.e., in the Sredinny and Kankaren ranges).

351 In conclusion, our model results imply that irrespective of the annual temperature range ( $\Delta T_a$   
352 LGM i.e. a reduction in winter temperature) or glacier type (DDF) used, annual precipitation in  
353 Pacific Russia during the gLGM must have been similar to, or even exceeded, modern values  
354 if summers were as warm as present while mountain glaciers were more extensive than today  
355 (reaching the sizes suggested by Barr and Clark, 2011).

356

## 357 *5.2. Comparison with proxy data*

358 Unfortunately, an assessment of whether precipitation on Kamchatka during the gLGM was  
359 similar to, or even greater than, today cannot be made on the basis of independent proxy-data,  
360 since such information is not available (Dirksen et al., 2013). In the Kankaren Range, pollen-  
361 based climate reconstructions provide evidence for the former presence of snow-bed plant-  
362 communities thereby indicating abundant snow-accumulation during the gLGM (Lozhkin and  
363 Anderson, 2013; Anderson and Lozhkin, 2015), a finding generally in concert with the  
364 presence of glaciers and abundant precipitation. On the other hand, pollen assemblages also  
365 contrast with our findings, as the paucity of shrubs in the Kankaren region points to reduced  
366 moisture availability, relative to today (Lozhkin and Anderson, 2013; Anderson and Lozhkin,  
367 2015). One possibility to explain discrepancies between DDM results and the pollen-  
368 interpretation is that aridity persisted in the Kankaren Range at the gLGM, despite increased  
369 precipitation, as moisture may have been trapped in glaciers and ground ice (Sergin and

370 Scheglova, 1976; Alfimov and Berman, 2001), meaning that precipitation, even if abundant,  
371 may not have been available to plants.

372 Nevertheless, there are good environmental reasons to expect increased aridity through reduced  
373 precipitation in the Siberian interior as well as along the Pacific coast during the gLGM. For  
374 example, the growth of ice-sheets elsewhere in the Northern Hemisphere is presumed to have  
375 deprived NE Russia of moisture (e.g. Seigert et al., 2001; Stauch and Gualtieri,  
376 2008). Moreover, during this period, the Bering and Chukchi-Shelves were exposed, reducing  
377 marine influences in western and central Beringia (Laukhin et al., 2006; Yanase and Abe-  
378 Ouchi, 2007; Barr and Clark et al., 2011). In addition, proxy-based studies point to extensive  
379 sea-ice coverage (Sakamoto et al., 2005; Caissie et al., 2010; Smirnova et al., 2014) which also  
380 suggests that winter sea surface temperatures were lower than at present. These factors would  
381 reduce evaporation over the marginal N-Pacific (Sancetta, 1983) and are supported by  
382 paleoclimate modelling studies which find no indication of increased precipitation in the N  
383 Pacific realm during the gLGM (Yanase and Abe-Ouchi, 2007), but do indicate reduced annual  
384 precipitation (by ~ 30–60%; Budiko et al., 1992; Velichko, 1993; Yanase and Abe-Ouchi,  
385 2007). Also, further north in the Pacific Sector (Anadyr Lowlands; area of Pekulney  
386 Mountains, Fig. 1A) as well as in the non-Pacific Sector (Fig. 1A), pollen point to increased  
387 aridity during the gLGM (Sher et al., 2005; Kienast et al., 2005; Lozhkin et al., 2007; Andreev  
388 et al., 2011; Lozhkin and Anderson, 2013). It therefore appears that existing paleo-  
389 environmental indicators generate a palaeoclimatic scenario for the NW Pacific realm, whereby  
390 extensive mountain glaciation, warm summers and arid conditions coexisted. This contrasts the  
391 findings from the DDM. The disagreement between the DDM results and climate indicators  
392 from the Siberian North may be explained by a strong precipitation gradient with wet  
393 conditions along the coast and very dry conditions in the interior. Such a gradient is reflected  
394 by the gLGM glacier extent in Siberian Mountain Ranges, as Barr and Clark (2012) noted that

395 during the gLGM glaciers were largest in the coastal areas (i.e. Kamchatka and the Koryak  
396 Range) and became smaller in mountain ranges further inland (e.g. Anyuy and Pekulney  
397 Mountains). The Verkhoyansk Mountains (centred on  $\sim 67^{\circ}\text{N}$ ,  $127^{\circ}\text{E}$ ) even appear to have  
398 remained largely ice free during the gLGM (Stauch and Gualtieri, 2008; Stauch and Lehmkuhl,  
399 2010; Zech et al., 2011; Barr and Clark, 2012). Furthermore, palaeobotanical evidence  
400 indicates that Beringia was a mosaic of different vegetation regimes during the gLGM (e.g.  
401 Elias and Crocker, 2008; Kuzmina et al., 2011 Anderson and Lozhkin, 2015 and references  
402 therein), and this may reflect a variety of climate zones that vary with respect to temperature  
403 and moisture. However, concerning the Pacific Sector of Siberia, this picture consisting of  
404 warm summers, reduced precipitation and extensive mountain glaciation appears to contradict  
405 inferences made from the DDM approach adopted here. As such, the assertion that extensive  
406 glaciers and warm summer temperatures coincided in Pacific NE Russia at the gLGM may be  
407 brought into question.

408 Uncertainties in the chronologies of either temperature or glaciation proxies may explain the  
409 discrepancies; yet the chronology for the marine sediment-core (dated by  $^{14}\text{C}$  of planktic  
410 foraminifera and by core-to-core correlations of XRF data from a set of sediment cores  
411 obtained from the Bering Sea and the NW Pacific) on which the temperature record for  
412 Kamchatka was established accurately defines the gLGM (Max et al., 2012; Meyer et al.,  
413 2016a, b). Also, studies which indicate that in western Beringia and the on the BLB summers  
414 during the gLGM were as warm as (or even warmer than) today, are based on soil sequences  
415 in which the gLGM is well constrained by radiocarbon dating of plant remains, insects and  
416 mammal bones (Elias, 2001; Kienast et al., 2005; Sher et al., 2005). In terms of glaciation, a  
417 small number of radiocarbon dates from the Sredinny Mountains suggest deglaciation prior to  
418 10-21 ka. When calibrated using the IntCal13 calibration curve (Reimer et al., 2013) and  
419 CALIB 7.1 program (Stuiver et al., 2016), this age range extends to 9.6-23.4 ka BP. On this

420 basis, moraines in the Sredinny Mountains, and the glacier reconstruction of Barr and Clark  
421 (2011), are assigned to the gLGM (18-24 ka BP; Braitseva et al., 1968; Melekestsev et al.,  
422 1970; Stauch and Gualtieri, 2008; Barr and Clark, 2016). Similarly, cosmogenic dating ( $^{36}\text{Cl}$ )  
423 from the Koryak and Kankaren Ranges suggest exposure (i.e., deglaciation) between 10.62 and  
424 21.65 ka, again constraining the glacier reconstruction of Barr and Clark (2011) to the gLGM  
425 (i.e. 18-24 ka BP). Though online tools allow  $^{36}\text{Cl}$  ages to be re-calibrated (e.g., CRONUScalc;  
426 Marrero et al., 2016), this procedure relies on the original reporting of detailed methodological  
427 and laboratory information (e.g. latitude, longitude, elevation, sample thickness, sample  
428 density, topographic shielding correction factor, CN production rates, scaling factors) (Small  
429 et al., 2016). Without this information legacy data cannot be updated to reflect the current state  
430 of knowledge and its overall reliability is ambiguous (cf. Small et al. 2016). Unfortunately, for  
431 the Gualtieri et al. (2000) data, the required information is unavailable, and we therefore  
432 report  $^{36}\text{Cl}$  ages as originally published (e.g., Small et al., 2016) while acknowledging that any  
433 inferences drawn must be treated with appropriate caution. Fortunately, a supporting  
434 chronology for the terrestrial  $^{14}\text{C}$  and  $^{36}\text{Cl}$  ages is provided by sediment cores from the NW  
435 Pacific which indicate that ice rafted debris (IRD), originating from the Kamchatka Peninsula  
436 (St John and Krissek, 1999), was continuously deposited throughout Marine Isotope Stage  
437 (MIS 2; i.e. 14-29 ka BP) and only ceased c.14-15 ka BP (St. John and Krissek, 1999; Kiefer  
438 et al., 2001; Bigg et al., 2008; Gebhardt et al., 2008). In these records, the gLGM is well  
439 constrained by radiocarbon dated foraminifera (e.g Kiefer et al., 2001; Gebhardt et al., 2008).  
440 Thus, the IRD records suggest that outlet glaciers from the eastern coast of Kamchatka  
441 terminated in the NW Pacific during the gLGM and that ice retreat did not occur until c.15 ka  
442 BP. This supports the terrestrial chronology, which suggests that the reconstruction of Barr and  
443 Clark (2011) (Fig. 1B) represents ice extent at the gLGM (18-24 ka BP). As a consequence,  
444 the coexistence of warm summers and extensive mountain glaciation at the gLGM is

445 considered likely and uncertainties in either the glacial or the temperature chronology fail to  
446 fully account for the discrepancies between several environmental indicators noted in this  
447 paper. Hence, the view of abundant precipitation in the Pacific Sector of Siberia during the  
448 gLGM is supported.

449

### 450 *5.3. Possible mechanisms for abundant annual precipitation at the gLGM*

451 Meyer et al. (2016a) suggested that the warm summers on Kamchatka resulted from stronger-  
452 than-present southerly winds over the subarctic NW Pacific due to a strengthening, or westward  
453 displacement, of the NPH. Besides summer warming, increased advection of maritime air  
454 masses from the south simultaneously leads to more precipitation during the summer months  
455 in southeast Siberia, as summarized in the climate synopsis for Beringia by Mock et al. (1998).  
456 Given this interpretation, the temperature record may be an indirect indication for wetter-than-  
457 present conditions in Pacific Siberia during the summer season. Unfortunately, no direct proxy-  
458 based reconstructions of gLGM precipitation are available, so this assumption remains to be  
459 tested. Increased precipitation in the summer months contrasts with several studies utilising  
460 General Circulation Models, which predict that summer precipitation in East Asia was  
461 significantly reduced during the gLGM (Yanase and Abe-Ouchi, 2007). To explain this  
462 reduction, Yanase and Abe-Ouchi (2007) suggested two underlying mechanisms: (I) weakened  
463 advection of maritime air masses to the East Asian coast in response to a weakened NPH. (II)  
464 A reduction of precipitable moisture as a consequence of reduced evaporation over the NW  
465 Pacific due to lowered SST. (I) can be challenged by the proxy-based inference for increased  
466 southerly flow over Kamchatka (Meyer et al. 2016a). However, (II) seems to be a robust  
467 scenario since various SST records from the open North Pacific (south of 50°N) show lowered  
468 temperature during the LGM (e.g. Harada et al., 2012). However, in the marginal NW Pacific,  
469 in the vicinity of Kamchatka (site 12KL, Fig. 1A), summer SST during the LGM was probably

470 only 1°C lower than at present (Meyer et al., 2016b), thereby giving reason to assume the NW  
471 Pacific was free of sea ice during LGM summers. Given relatively warm SST and limited sea-  
472 ice extent, evaporation over the subarctic NW Pacific may not have differed significantly from  
473 present. Considering alkenone-based SST records, the same may have applied for the Sea of  
474 Okhotsk, since these records suggest that glacial temperatures in the area were similar to  
475 present (Seki et al., 2004; Harada et al., 2012). However, these records are assumed to be biased  
476 by shifting production-seasons of the alkenone-producing coccolithophores (e.g. Seki et al.,  
477 2004, 2009), a hypothesis which is supported by SST reconstructions based on TEX<sup>L</sup><sub>86</sub>-  
478 paleothermometry which indicate a cooling of ~ 5°C relative to modern (Harada et al., 2012;  
479 Seki et al., 2014). Nevertheless, in the subarctic NW Pacific, minor changes in evaporation  
480 (between gLGM and present) combined with increased southerly winds during the summer  
481 months may have resulted in abundant precipitation in the Pacific sector of Siberia at the  
482 gLGM.

483

#### 484 *5.4. Implications for glacier growth in NE Russia at the gLGM*

485 The conclusions of chapter 5.3 suggest that summer precipitation may have mainly accounted  
486 for the precipitation necessary to sustain glaciers in the Pacific Sector during the gLGM. As  
487 noted in section 4, results from the DDM do not directly include precipitation during the  
488 ablation season, as this is presumed to largely fall as rain at the ELA (and therefore not  
489 contribute to glacial accumulation). However, it is possible that precipitation above the ELA  
490 fell as snow even during summer months, and thereby contributed to the glacier growth.  
491 Additional, the ablation season (number of positive degree days) was likely shorter than today,  
492 as suggested by our simulations for the annual temperature cycle during the gLGM (see Fig.  
493 3). A short ablation season may have supported glacier stability by limiting total annual  
494 ablation. Also, colder winters in combination with polar-type glaciers explain why glaciers

495 were more extensive than today while at the gLGM precipitation and summer temperature were  
496 similar than at present.

497 By indicating that annual precipitation in Pacific Russia during the gLGM must have been as  
498 abundant as today or even exceeded the modern values if summers were as warm as present  
499 while mountain glaciers were more extensive than today, the DDM-results from the present  
500 study suggest that warm summer temperatures limited gLGM glacier growth in south-eastern  
501 Pacific Siberia. Interestingly, DDM-derived estimates for glacial precipitation in the Pekulney  
502 Mountains (north of the Anadyr-Lowlands, 66.09°N, 175.10°E, Fig. 1A) from Barr and Clark  
503 (2011) suggest that precipitation must have exceeded modern values, although gLGM summer  
504 temperature was estimated to have been 3.1-4.1°C lower than at present (Alfimov and Berman,  
505 2001; Barr and Clark, 2011). This finding suggests that also in the north-eastern Pacific Sector  
506 summer temperature may have limited glacier growth. However, Barr and Clark (2011)  
507 acknowledged that gLGM temperature reconstructions for the Pekulney area vary considerably  
508 (Alfimov and Berman, 2001; Lozhkin et al., 2007; Barr and Clark, 2011), and calculations  
509 based on a 6.4°C reduction in  $T_{\text{July}}$  (Lozhkin et al., 2007), would suggest that annual LGM  
510 accumulation was below the modern mean, supporting that aridity hampered glacier growth at  
511 the gLGM (Brigham-Grette et al., 2003; Stauch and Gualtieri, 2008; Barr and Clark, 2011;  
512 Barr and Spagnolo, 2013). Therefore, Barr and Clark (2011) considered the first scenario  
513 unlikely. In light of our findings, and with evidence for warm gLGM summers being  
514 widespread in Siberia (Alfimov and Berman, 2001; Elias, 2001; Kienast et al., 2005; Sher et  
515 al., 2005; Berman et al., 2011; Meyer et al., 2016 a), the relatively high precipitation estimates  
516 may now appear more likely. As such, and despite the ambiguity in the Pekulney Mountains,  
517 the DDM-derived precipitation estimates for the three mountain ranges (the Sredinny,  
518 Kankaren and Pekulney) emphasize that summer temperature may have been an important  
519 limiting factor for glacier growth in the Pacific Sector of Siberia at the gLGM. This contrasts



520 with the prevailing view that glacier expansion in NE Russia was hampered by increased aridity  
521 (Seigert et al., 2001; Brigham-Grette et al., 2003; Stauch and Gualtieri, 2008; Barr and Clark,  
522 2011; Barr and Spagnolo, 2013), at least regarding the Pacific Sector. Since proxies suggest  
523 that extreme arid conditions prevailed due to increased continentality in interior Siberia (e.g.  
524 Guthrie et al., 2001; Kienast et al., 2005; Sher et al., 2005; Lozhkin et al., 2007), the aridity  
525 hypothesis may apply to regions in continental Siberia.

526

## 527 **6. Summary and Conclusion**

528 There is consensus that the local LGM in NE Russia preceded the gLGM, occurring around 40  
529 ka BP and that glaciers shrank towards the gLGM. At the gLGM glaciation was restricted to  
530 mountain glaciers in Siberian mountain ranges, such as the Sredinny (Kamchatka) and the  
531 Kankaren Range. Evidence exists to suggest that during the gLGM, summers in Kamchatka  
532 and the Kankaren Range were as warm as at present while mountain glaciation was more  
533 extensive than today. As a result, we hypothesized that, during this period, precipitation must  
534 have been abundant (at least comparable to present) and that summer temperature was an  
535 important limiting factor for ice-sheet growth in the Pacific Sector of NE Russia. Our DDM-  
536 results support this hypothesis indicating that despite a reduction in winter temperatures, annual  
537 precipitation at the gLGM, was similar to, or higher than the modern mean, depending on  
538 whether glaciers were of polar or temperate type. In the Pacific Sector precipitation may have  
539 been increased relative to today due to stronger southerly winds during the summer season and  
540 relatively warm SST in the marginal NW Pacific, and this may have resulted in heavy snowfall  
541 above the ELA, allowing glaciers to develop and persist despite warm summer temperatures.  
542 Additionally the ablation season may have been notably short, thereby limiting total ablation.  
543 However, the majority of paleo-environmental indicators from interior and Pacific Siberia as  
544 well as the subarctic N Pacific point to dryer-than-present conditions in continental Siberia and

545 the Pacific Sector at the gLGM. This is why it is generally assumed that strong aridity restricted  
546 glaciation in NE Russia during the gLGM, an idea our findings are in contrast with.  
547 Discrepancies with interior Siberia may be due to pronounced regional differences in Beringian  
548 climate with wet conditions in maritime Siberia and severe dryness in farther inland. Thus,  
549 strong aridity potentially inhibited glacier growth in continental Siberia while summer  
550 temperature restricted glacier expansion in regions bordering the Pacific coast. Discrepancies  
551 in the Pacific Sector together with the sparseness of independent proxy data for precipitation  
552 in this region highlight the need of further investigations of Beringian palaeo-climate through  
553 the last glacial cycle.

554

#### 555 **Acknowledgements**

556 This study was conducted within the frame of a PhD-project which was funded by the by the  
557 Helmholtz association through the President's Initiative and Networking Fund. GLOMAR –  
558 Bremen Graduate School for Marine Sciences is thanked for funding V. Meyer's research stay  
559 at Queen's University Belfast which allowed the realization of the project. The staff of the  
560 department of Geography, Archaeology and Paleoecology at Queen's University Belfast are  
561 thanked for their kind support during the research stay. We are also grateful to Phil Hughes and  
562 Julie Brigham-Grette for their detailed and constructive reviews.

563

#### 564 **References**

565 Alfimov, A.V., Berman, D.I., 2001. Beringian climate during the late Pleistocene and  
566 Holocene. *Quat. Sci. Rev.* 20, 127–134.

- 567 Ananicheva, M. D., Krenke, A. N., Hanna, E., 2008. Mountain glaciers of NE Asia in the near  
568 future: a projection based on climate-glacier systems interaction. *Cryosphere Discussion*,  
569 2, 1-21.
- 570 Anderson, P. A., and Lozhkin, A. V., 2015. Late Quaternary vegetation of Chukotka (Northeast  
571 Russia), implications for Glacial and Holocene environments of Beringia. *Quat. Sci. Rev.*  
572 107, 112-128.
- 573 Andreev, A. A., Schirmer, L., Tarasov, P. E., Ganopolski, A., Brovkin, V., Siebert, C., ...  
574 Hubberten, H. W., 2011. Vegetation and climate history in the Laptev Sea region (Arctic  
575 Siberia) during Late Quaternary inferred from pollen records. *Quat. Sci. Rev.*, 30, 2182–  
576 2199. <http://doi.org/10.1016/j.quascirev.2010.12.026>
- 577 Arkhipov, S.A., Isaeva, L.L., Bepaly, V.G., Glushkova, O.Y., 1986. Glaciation of Siberia and  
578 North-East USSR. *Quat. Sci. Rev.* 5, 463–474.
- 579 Barr, I.D., Clark, C.D., 2011. Glaciers and climate in Pacific Far NE Russia during the Last  
580 Glacial Maximum. *J. Quat. Sci.* 26, 227–237.
- 581 Barr, I.D., Clark, C.D., 2012. Late Quaternary glaciations in Far NE Russia: combining  
582 moraines, topography, and chronology to assess regional and global glaciation synchrony.  
583 *Quat. Sci. Rev.* 53, 72–87.
- 584 Barr, I.D., Solomina, O., 2014. Pleistocene and Holocene glacier fluctuations upon the  
585 Kamchatka Peninsula. *Glob. Planet. Change*, 1–11.
- 586 Barr, I.D., Spagnolo, M., 2013. Paleoglacial and Paleoclimatic conditions in the NW Pacific,  
587 as revealed by a morphometric analysis of cirques on the Kamchatka Peninsula.  
588 *Geomorphology*, 192, 15–29.

- 589 Berman, D., Alfimov, A., Kuzmina, S., 2011. Invertebrates of the relict steppe ecosystems of  
590 Beringia, and the reconstruction of Pleistocene landscapes. *Quat. Sci. Rev.* 30, 2200–  
591 2219.
- 592 Bigg, G. R., Clark, C. D., Hughes, A. C. L., 2008. A last glacial ice sheet on the Pacific Russian  
593 Coast and catastrophic change arising from coupled ice-volcanic interactions. *Earth Planet*  
594 *Sci. Lett.*, 265, 559-570.
- 595 Braithwaite R. J, Raper, S. C. B, Chutko, K., 2006. Accumulation at the equilibrium line  
596 altitude of glaciers inferred from a degree–day model and tested against field observations.  
597 *Annals of Glaciology*, 43, 329–334.
- 598 Brigham-Grette, J., Gualtieri, L. M., Glushkova, O. Yu., Hamilton, T.D., Mostoller, D., Kotov,  
599 A., 2003. Chlorine-36 and <sup>14</sup>C chronology support a limited last glacial maximum across  
600 central Chutotka, north-eastern Siberia, and no Beringian ice sheet. *Quat. Res.* 59, 386–  
601 398.
- 602 Brugger, K.A., 2006: Late Pleistocene climate inferred from the reconstruction of the Taylor  
603 River glacier complex, southern Sawatch Range, Colorado. *Geomorphology*, 75: 318-  
604 329.
- 605 Budiko, M.I., Borzenkova, I.I., Menzhulin, G.B., Selyakov, K.I., 1992. Expecting changes of  
606 regional climate. *Izvestiya AN SSSR, Series Geographica*, 4, 36-52 (in Russian).
- 607 Caissie, B.E., Brigham-Grette, J., Lawrence, K.T., Herbert, T.D., Cook, M.S., 2010. Last  
608 Glacial Maximum to Holocene sea surface conditions at Umnak Plateau, Bering Sea, as  
609 inferred from diatom, alkenone, and stable isotope records. *Paleoceanography* 25,  
610 PA1206.

611 Climate data from Klyuchi climate station. <http://de.climate-data.org/location/284590/>  
612 (checked September 2015)

613 Climate data from Petropawlowsk Kamtschatski climate station. <http://de.climate->  
614 [data.org/location/1810/](http://de.climate-data.org/location/1810/) (checked October 2015)

615 Climate data from Alkatvaam climate station. <http://de.climate-data.org/location/284590/>  
616 (checked March 2016).

617 Climate data from Meynypilgyno climate station. <http://de.climate-data.org/location/284590/>  
618 (checked March 2016).

619 Dirksen, V., Dirksen, O., Diekmann, B., 2013. Holocene vegetation dynamics and climate  
620 change in Kamchatka Peninsula, Russian Far East. *Rev. Paleobot. Palynol.* 190, 48–65.

621 Elias, S.A., 2001. Mutual climatic range reconstructions of seasonal temperatures based on  
622 Late Pleistocene fossil beetle assemblages in eastern Beringia. *Quat. Sci. Rev.* 20, 77–91.

623 Elias, S., Crocker, B., 2008. The Bering Land Bridge: a moisture barrier to the dispersal of  
624 steppe–tundra biota? *Quat. Sci. Rev.*, 27(27–28), 2473–2483.  
625 <http://doi.org/10.1016/j.quascirev.2008.09.011>

626 Felzer, B., 2001. Climate impacts of an ice sheet in East Siberia during the Last Glacial  
627 Maximum. *Quat. Sci. Rev.* 20, 437–447.

628 Gebhardt, H., M. Sarnthein, P. M. Grootes, T. Kiefer, H. Kuehn, F. Schmieder, U. Röhl, (2008),  
629 Paleonutrient and productivity records from the subarctic North Pacific for Pleistocene  
630 glacial terminations I to V. *Paleoceanography*, 23, PA4212 doi:10.1029/2007PA001513.

- 631 Glushkova, O. Yu., 2001. Geomorphological correlation of Late Pleistocene glacial complexes  
632 of Western and Eastern Beringia. *Quat. Sci. Rev.* 20, 405–417.
- 633 Grosswald MG. 1988. An Antarctic-style ice sheet in the Northern Hemisphere: towards a new  
634 global glacial theory. *Polar Geography and Geology*, 12, 239–267.
- 635 Grosswald, M. G. 1998. Late Weichselian ice sheets in Arctic and Pacific Siberia. *Quat. Int.*  
636 45/46, 3–18.
- 637 Grosswald, M. G., Hughes, T.J., 2002. The Russian component of an Arctic Ice Sheet during  
638 the Last Glacial Maximum. *Quat. Sci. Rev.* 21, 121–146.
- 639 Grosswald, M. G., Hughes, T.J., 2005. “Back-arc” marine ice sheet in the Sea of Okhotsk. *Rus.*  
640 *J. Earth. Sci.* 7. doi:10.2205/2005ES000180.
- 641 Grosswald, M. G., Kotlyakov, V. M., 1969. Present-day glaciers in USSR and some data on  
642 their mass balance. *J. Glaciol.* 8, 9-21.
- 643 Gualtieri, L., Glushkova, O., Brigham-Grette, O. J., 2000. Evidence for restricted ice extent  
644 during the last glacial maximum in the Koryak Mountains of Chukotka, far eastern Russia.  
645 *Geol. Soc. Amer. Bull.* 112, 1106–1118.
- 646 Gualtieri, L., Vartanyan, S., Brigham-Grette, J., Patricia, M., Anderson, P.M., 2003.  
647 Pleistocene raised marine deposits on Wrangel Island, NE Siberia: implications for Arctic  
648 ice sheet history. *Quat. Res.* 59, 399–410.
- 649 Guthrie, R. D., 2001. Origin and causes of the mammoth steppe: a story of cloud cover, woolly  
650 mammal tooth pits, buckles, and inside-out Beringia. *Quat. Sci. Rev.*, 20, 549–574.

651 Harada, N., Sato, M., Seki, O., Timmermann, A., Moossen, H., Bendle, J., Nakamura, Y.,  
652 Kimoto, K., Okazaki, Y., Nagashima, K., Gorbarenko, S. a., Ijiri, A., Nakatsuka, T.,  
653 Menviel, L., Chikamoto, M.O., Abe-Ouchi, A., Schouten, S., 2012. Sea surface  
654 temperature changes in the Okhotsk Sea and adjacent North Pacific during the last glacial  
655 maximum and deglaciation. *Deep Sea Res. Part II Top. Stud. Oceanogr.* 61-64, 93–105.

656 Hughes, P. D. (2008). Response of a Montenegro glacier to extreme summer heatwaves in 2003  
657 and 2007. *Geografiska Annaler, Series A*, 90(4), 259-267. DOI: 10.1111/j.1468-  
658 0459.2008.00344.x.

659 Hughes, P. D., 2009. Loch Lomond Stadial (Younger Dryas) glaciers and climate in Wales.  
660 *Geol. J.*, 44, 375–391.

661 Hughes, P. D., and Braithwaite, R. J., 2008. Application of a degree-day model to reconstruct  
662 Pleistocene glacial climates. *Quat. Res.* 69, 110–116.

663 Ivanov, A., 2002. The Far East. In: *The Physical Geography of Northern Eurasia*,  
664 Shahgedanova M. (ed.). Oxford University Press: Oxford, 422-447.

665 Jones, V., and Solomina, O., 2015. The geography of Kamchatka. *Glob. Plan. Change*, 134, 3-  
666 9.

667 Kern, Z., László, P., 2010. Size specific steady-state accumulation-area ratio: an improvement  
668 for equilibrium-line estimation of small palaeoglaciers. *Quat. Sci. Rev.* 29, 2781–2787.

669 Kienast, F., Schirmer, L., Siegert, K., Tarasov., P., 2005. Paleobotanical evidence for warm  
670 summers in the East Siberian Arctic during the last cold stage. *Quat. Res.* 63, 283-300.

- 671 Kim, S.-J., Crowley, T. J., Erickson, D. J., Govindasami, B., Duffy, P. B., Lee, B. Y., 2008.  
672 High-resolution climate simulation of the last glacial maximum. *Clim. Dyn.*, 31, 1-16.
- 673 Kuzmina, S. A., Sher, A. V., Edwards, M. E., Haile, J., Yan, E. V., Kotov, A. V., &  
674 Willerslev, E. (2011). The late Pleistocene environment of the Eastern West Beringia  
675 based on the principal section at the Main River, Chukotka. *Quat. Sci. Rev.*, 30, 2091–  
676 2106. <http://doi.org/10.1016/j.quascirev.2010.03.019>
- 677 Laukhin, S. A., Zhimin, J., Pushkar, V. S., Cherepanova, M. V., 2006. Last Glaciation in the  
678 northern part of the Eastern Chukchi Peninsula and paleoceanography of the North  
679 Pacific. *Dokl. Earth Sci.*, 441A, 1422-1426.
- 680 Laumann, T., Reeh, N., 1993. Sensitivity to climate change of the mass balance of glaciers in  
681 southern Norway. *Journal of Glaciology* 39, 656–665.
- 682 Lozhkin, A. V., Anderson, P. M., Matrosova, T. V., Minyuk, P. S., 2007. The pollen record  
683 from El'gygytgyn Lake: Implications for vegetation and climate histories of northern  
684 Chukotka since the late middle Pleistocene. *J Paleolimnol*, 37(1), 135–153.  
685 <http://doi.org/10.1007/s10933-006-9018-5>
- 686 Lozhkin, A. V., Anderson, P. M., 2013. Late Quaternary records from the Anadyr Lowland,  
687 central Chukotka (Russia). *Quat. Sci. Rev.*, 68, 1-16.
- 688 Lynch, C., Barr, I.D., Mullan, D., Ruffell, A., 2016. Rapid glacial retreat on the Kamchatka  
689 Peninsula during the early 21<sup>st</sup> Century. *The Cryosphere* 10, 1809–1821.
- 690 Marrero, S.M., Phillips, F.M., Borchers, B., Lifton, N., Aumer, R., Balco, G., 2016.  
691 Cosmogenic nuclide systematics and the CRONUScal program. *Quaternary*  
692 *Geochronology* 31, 160–187.



- 693 Melekestsev, I.V., Braitseva, O. A, Kraevaya, T.S.,1970. Application of the complex  
694 techniques to determine the age of Quaternary volcanic formations (in the case of  
695 Kamchatka). *Izv AN SSSR Set Geol.* 10, 149-153 (in Russian).
- 696 Meyer, H., Dereviagin, A., Siegert, C., Hubberten, H.-W., 2002. Paleoclimate studies on  
697 Bykovsky Peninsula, North Siberia - hydrogen and oxygen isotopes in ground ice.  
698 *Polarforschung* 70, 37–51.
- 699 Meyer, V. D., Lohmann, G., Hefter, J., Tiedemann, R., Mollenhauer, G., 2016 a. Development  
700 of summer temperature on the Kamchatka Peninsula, Russian Far East, over the past  
701 20,000 years. *Clim. Past Discuss.*, doi:10.5194/cp-2016-21, in review.
- 702 Meyer, V. D., Max, L., Hefter, J., Tiedemann, R., Mollenhauer, G., 2016 b. Glacial-to-  
703 Holocene evolution of sea surface temperature and surface circulation in the subarctic  
704 Northwest Pacific and the Western Bering Sea. *Paleoceanography* 31, 916-927,  
705 doi:10.1002/2015PA002877.
- 706 Mix, A. C., Bard, E., Schneider, R., 2001. Environmental processes of the ice age: land, ocean,  
707 glaciers (ELIPOG). *Quat. Sci. Rev.*, 20, 627-657.
- 708 Mock, C.J., Mock, C.J., Bartlein, P.J., Bartlein, P.J., Anderson, P. A, Anderson, P. A, 1998.  
709 Atmospheric circulation patterns and spatial climatic variations. *Beringia. Int. J. Climatol.*  
710 10, 1085–1104.
- 711 Reimer, P.J., Bard, E., Bayliss, A., Beck, J.W., Blackwell, P.G., Bronk Ramsey, C., Buck, C.E.,  
712 Cheng, H., Edwards, R.L., Friedrich, M., Grootes, P.M., 2013. IntCal13 and Marine13  
713 radiocarbon age calibration curves 0-50,000 years cal BP. *Radiocarbon* 55(4), 1869–1887.

- 714 Ohmura A, Kasser P, Funk M. 1992. Climate at the equilibrium line of glaciers. *Journal of*  
715 *Glaciology* 3, 397–411.
- 716 Sakamoto, T., Ikehara, M., Aoki, K., Iijima, K., Kimura, N., Nakatsuka, T., Wakatsuchi, M.,  
717 2005. Ice-rafted debris (IRD)-based sea-ice expansion events during the past 100 kyrs in  
718 the Okhotsk Sea. *Deep Sea Res. Part II* 52 (16-18), 2275-2301.
- 719 Sancetta, C., 1983. Effect of Pleistocene glaciation upon oceanographic characteristics of the  
720 North Pacific Ocean and the Bering Sea. *Deep Sea Res.*, 30, 851-869.
- 721 Seki, O., Bendle, A. J., Harada, N., Kobayashi, N. Sawada, K., Moossen, H., Inglis, G. N.,  
722 Nagao, S., Sakamoto, T., 2014. Assessment and calibration of TEX<sub>86</sub> paleothermometry  
723 in the Sea of Okhotsk and the sub-polar North Pacific region: Implications for  
724 paleoceanography. *Progr. Oceanogr.*, 126, 254-266.
- 725 Seki, O., Kawamura, K., Ikehara, M., Nakatsuka, T., Oba, T., 2004. Variation of alkenone sea  
726 surface temperature in the Sea of Okhotsk over the last 85 kyrs. *Org. Geochem.*, 35, 347-  
727 354.
- 728 Seki, O., Sakamoto, T., Saki, S., Schouten, S., Hopmans, E., C., Sinningh Damsté, J. S.,  
729 Pancost, R. D., 2009. Large changes in sea ice distribution and productivity in the Sea of  
730 Okhotsk during the deglaciations. *Geochem., Geophys., Geosyst.*, 10, Q10007.
- 731 Sergin, S. Ya., Scheglova, M.S., 1976. Beringia climate during ice ages as result of influence  
732 of global and local factors. In: *Beringia in the Cenozoic*. Nauka Press, Vladivostok, pp.  
733 171-175 (in Russian).
- 734 Siegert, M.J., Dowdeswell, J.A., Hald, M., Svendsen, J., 2001. Modelling the Eurasian Ice  
735 Sheet through a full (Weichselian) glacial cycle. *Global Planet. Change* 31, 367–385.

- 736 Shahgedanova M., Perov, V., Mudriv, Y. 2002. In: The Physical Geography of Northern  
737 Eurasia, Shahgedanova M. (ed.). Oxford University Press: Oxford, 284-313.
- 738 Sher, A. V., Kuzmina, S. A., Kuznetsova, T. V. and Sulerzhitsky, L. D., 2005. New insights  
739 into the Weichselian environment and climate of the East Siberian Arctic, derived from  
740 fossil insects, plants, and mammals, *Quat. Sci. Rev.*, 24(5-6), 533–569,  
741 doi:10.1016/j.quascirev.2004.09.007.
- 742 Small, D., Clark, C.D., Chiverrell, R.C., Smedley, R.K., Bateman, M.D., Duller, G.A.T., Ely,  
743 J.C., Fabel, D., Medialdea, A., Moreton, S.G., 2016. Devising quality assurance  
744 procedures for assessment of legacy geochronological data relating to deglaciation of the  
745 last British-Irish Ice Sheet. *Earth-Science Reviews*, in press.  
746 doi:10.1016/j.earscirev.2016.11.007.
- 747 Smirnova, M. A., Kazarina, G. K., Matul, A. G. and Max, L., 2007. Diatom Evidence for  
748 Paleoclimate Changes in the Northwestern Pacific during the Last 20000 Years, *Mar.*  
749 *Geol.* 55(3), 425–431, doi:10.1134/S0001437015030157.
- 750 Solomina, O., Calkin, P., 2003. Lichenometry as applied to moraines in Alaska, USA, and  
751 Kamchatka, Russia. *Arct., Antarc., Apl. Res.*, 35, 129-143.
- 752 St. John, K.E., Krissek, L.A., 1999. Regional patterns of Pleistocene ice-rafted debris flux in  
753 the North Pacific. *Paleoceanography* 14, 653–662.
- 754 Stauch, G., and Gualteri, L., 2008. Late Quaternary Glaciations in northeastern Russia. *J.Quat.*  
755 *Sci.*, 23, 6-7.
- 756 Stauch, G., Lehmkuhl, F., 2010. Quaternary glaciations in the Verkhoyansk Mountains,  
757 Northeast Siberia. *Quaternary Research* 74, 145-155.

- 758 Stuiver, M., Reimer, P.J., Reimer, R.W., 2016. CALIB 7.1 [WWW program]. <http://calib.org>,  
759 (accessed: 10.12.16).
- 760 Velichko, A. A., 1993. North Eurasian landscape and climate development. The Late  
761 Pleistocene/Holocene: Elements of Forecast. Iss. I. Regional Paleogeography. Nauka  
762 Press, Moscow (in Russian).
- 763 Velichko, A.A., Wright, H.E., Barnosky, C.W., 1984. Late Quaternary Environments of the  
764 Soviet Union, University of Minnesota Press, Minneapolis.
- 765 Yanase, W. and Abe-Ouchi, A.: The LGM surface climate and atmospheric circulation over  
766 East Asia and the North Pacific in the PMIP2 coupled model simulations, *Clim. Past*,  
767 3(3), 439–451, doi:10.5194/cp-3-439-2007.
- 768 Zech, W., Zech, R., Zech, M., Leiber, K., Dippold, M., Frechen, M., Bussert, R., Andreev, A.,  
769 2011. Obliquity forcing of Quaternary glaciation and environmental changes in NE  
770 Siberia. *Quaternary International* 234, 133-145.